A Stacked FKM/PU Triboelectric Nanogenerator for Discrete Mechanical Energy Harvesting

Yuxiang Su, Anguo Liu, Wuwei Feng,* Yunqing Gu, Xiaonan Su, Guanyu Dai, Yilei Shao, Liping Wan, Haohan Fang, and Zhenhua Li*

| Read Online

ACCESS | Metrics & More | Article Recommendations | Supporting Information

ABSTRACT: To combine the advantages of elastic and nonelastic triboelectric materials, this work proposes a new type of triboelectric nanogenerator (TENG) based on stacking —the stacked FKM/PU TENG. By stacking the elastomer polyurethane (PU) and the nonelastomer fluororubber (FKM), the FKM/PU TENG combines the inherent triboelectric characteristics of both materials and the unique elasticity of PU to achieve an output performance that is much higher than that of the FKM-TENG or the PU-TENG. The maximum instantaneous open-circuit voltage and short-circuit current of the FKM/PU TENG reach 661 V and 71.2 μA, respectively. Under the limiting conditions of 3 Hz and maximum compression, this device can attain a maximum power density of 49.63 W/m^3 and light more than 500 LEDs. Therefore, stacking materials with different properties gives the FKM/PU TENG high output performance and great application potential, which can contribute to future development of discrete mechanical energy harvesting.
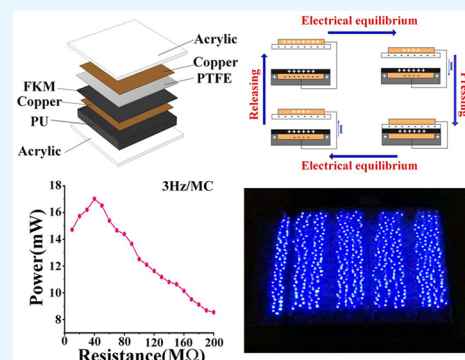
1. INTRODUCTION

Fossil energy has always been the most commonly used energy in the world, and it now faces a depletion crisis. However, abusing fossil fuels contaminates the environment and has an impact on human society that cannot be ignored.[1,2] Therefore, it is important to develop green energy and build clean energy-based systems to secure a better future. The triboelectric nanogenerator (TENG) was first presented by Zhonglin Wang at the Georgia Institute of Technology in 2012. Its principle is converting mechanical energy into electrical energy through triboelectrification and electrostatic induction.[3] It has been shown to have the advantages of high power density, high efficiency, lightweight, low cost, and simple manufacturing for collecting random and low-frequency mechanical energy.[4] The TENG uses the charge generated by the friction between two materials with different electronegativities to generate a potential difference, thereby driving electrons to move in the external circuit to form a current. TENGs can collect different kinds of mechanical energy such as vibration, rotation, swing, human motion,[5−8] wave,[9−11] and wind energy.[12−14]

There are mainly four TENG working modes: vertical contact separation, single electrode, independent layer, and sliding plane. Different modes are suitable for collecting mechanical energy in different forms and different motion environments, so TENGs are widely used in all aspects of life and production. Vertical contact separation is a common TENG working mode when different materials are placed between the two plates. The TENG output performance

increases when there is a greater discrepancy in electron-capturing ability between the triboelectric layers.[15] In 2020, Salauddin et al. proposed an MXene/Ecoflex nanocomposite with high negative electrical properties and mechanical stability. Made of nanocomposite and waterproof fabric, the TENG can achieve a much better maximum power density than the combination of PTFE and Nylon.[16] TENGs made of rigid materials cannot harvest mechanical energy well often because of the unsatisfactory contact and long-term wear on their surfaces. Therefore, researchers have tried to use elastic materials to fabricate TENGs. Liu et al. implanted conductive polyaniline nanowires (PANI NWs) on a polyurethane foam (PU) through simple dilute aniline chemical polymerization and constructed an ES-TENG.[17] Elastic deformation allows the TENG to respond effectively to random motions with different amplitudes and directions. However, elastic materials are triboelectrically weaker than rigid materials. Finding a method to integrate the characteristics of elastic and inelastic triboelectric materials would advance the TENG to a new level.
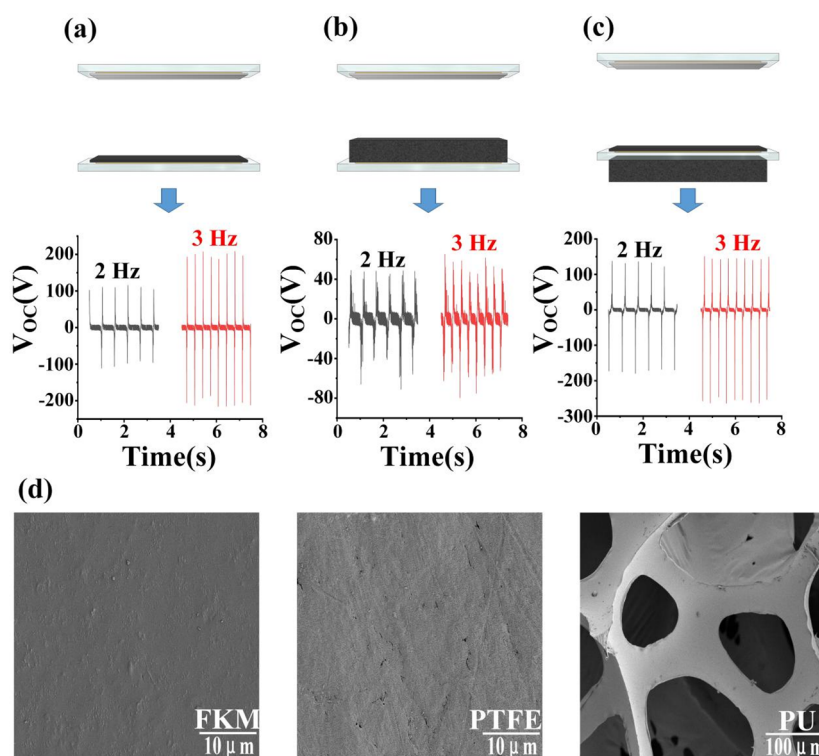
Figure 1. Structure and open-circuit voltage V_{OC} of the (a) FKM-TENG, (b) PU-TENG, and (c) FKM-TENG with a PU cushion. (d) Scanning electron microscopy images of the PU, FKM, and PTFE. FKM: fluororubber; TENG: triboelectric nanogenerator; PU: polyurethane; PTFE: polytetrafluoroethylene.

In this work, a stacked FKM/PU TENG is proposed and discussed, which is mainly composed of polytetrafluoroethylene (PTFE), fluororubber (FKM), PU, and conductive copper. The operation mode of contact separation is selected, and the stacked structure is divided into Plate A and Plate B. Plate A consists of PTFE and copper to form a common triboelectric generation unit. Plate B uses FKM as the direct triboelectric surface layer, and the PU is the bottom. The copper electrode is set between them. The PU is electropositive material and also involved in the electron transfer between FKM and PTFE when Plate A contacts and squeezes Plate B. Under continuous extrusion, PTFE obtains more electrons from FKM and PU. Moreover, adding an elastomer to the bottom of Plate B enhances the extrusion and the duration. The increased PU deformation enhances the output of Plate B. Compared with the traditional design of triboelectric nanogenerator, the stacked FKM/PU TENG effectively improves the adhesion and slows down the surface wear by using the stacking structure of different triboelectric materials. Besides, under the coupling effect of PU and FKM, more induced charges are generated on the conductive layer, and the output performance of the TENG is significantly improved. The stacked FKM/PU TENG can adapt to different extrusion environments and bring different output effects. In the maximum compression condition, the maximum open-circuit voltage, short-circuit current, instantaneous output power, the amount of transferred charge within 1 s and power density can reach 661 V, 71.2 μA, 2.23 μC, 17.02 mW, and 49.62 W/m^3, respectively. Furthermore, the TENG can easily light 540 commercial LEDs and support calculators for simple operations. This improved method of TENG is more economical, convenient and efficient without complicated material procession or charge implantation. Therefore, the

potency of this brand new triboelectric nanogenerator in mechanical energy collection deserves exploration.

2. EXPERIMENTAL SECTION

The stacked FKM/PU TENG is made of Plates A and B. Plate A is a simple triboelectric unit composed of substrate, PTFE sheet (area and thickness: 7 cm × 7 cm; 0.6 mm), and conductive copper tape. Plate B consists of an acrylic substrate, FKM sheet (7 cm × 7 cm; 1 mm), PU (7 cm × 7 cm; 1 cm; density: 40 PPI), and copper layer in a stacked structure that forms a unit with opposite triboelectric properties to those of Plate A. The FKM is on the top of Plate B and in direct contact with the PTFE of Plate A. The PU is under the FKM, and copper layer is arranged between them to lead out the wire. The areas of the conductive layers and substrates are 6.5 × 6.5 cm^2 and 8× 8 cm^2, respectively. Before stacked FKM/PU TENG is fabricated, the PTFE and FKM are successively placed in ethanol and deionized water and ultrasonically cleaned for 5 min.

A reciprocating mechanism provides external excitation for the TENG. It is set on the workbench, and the front end is fixed with Plate A, as shown in Figure S1 and Video S1. On the other side of the work table, a right-angle holder is used to set Plate B and reinforce it with nuts. Referring to the parameters in Table S1 provided by the manufacturer, the stroke of the reciprocating mechanism is 7 cm, the maximum rpm of the motor is 120, the and the pressure range is 0−4.2 N. The initial distance between Plates A and B is 8 cm.

To explore the electrical parameter of the TENG, a DMM6500 digital multimeter is used in this experiment. The NPLC is 0.0005 (acquisition period: 10 μs) to achieve the maximum sampling rate. The digital multimeter can better capture the peak output value of the stacked FKM/PU TENG.

2.1. Structure and Working Principle. Before studying the stacked structure, the performances of PU and FKM as individual triboelectric materials are observed. FKM and PU are electropositive materials according to the triboelectric series,[18] as shown in Figure 1a−c. Therefore, when each of the two comes into contact with PTFE, the FKM or PU surface electrons transfer to the PTFE surface. This makes the PTFE negatively charged and the FKM or PU positively charged. Because of the different material characteristics of FKM and PU, the FKM TENG has higher output voltage than the PU TENG at 2 and 3 Hz. However, PU as an elastomer has stronger adaptability and sensing potential in complicated environments.[17] Hence, we hope the FKM TENG will also have the characteristics of an elastomer. The triboelectric units of Plate B in Figure 1a−c are FKM-TENG, but the difference is that PU is added as the substrate in Figure 1c so that the TENG has the characteristics of elastic deformation in the process of contact separation, which makes the bonding time of FKM and PU effectively extended. Based on the transfer mechanism of induced charge, the TENG can generate a higher peak pulse voltage during extrusion. When released, the deformation recovery reduces the plate separation speed and cannot enhance the V_{OC}. The scanning electron microscopy images of the FKM, PTFE, and PU are shown in Figure 1d.

Therefore, to integrate the characteristics of the FKM-TENG and PU-TENG, the stacked structure is designed and illustrated as in Figure 2a. The PU is set below FKM, and
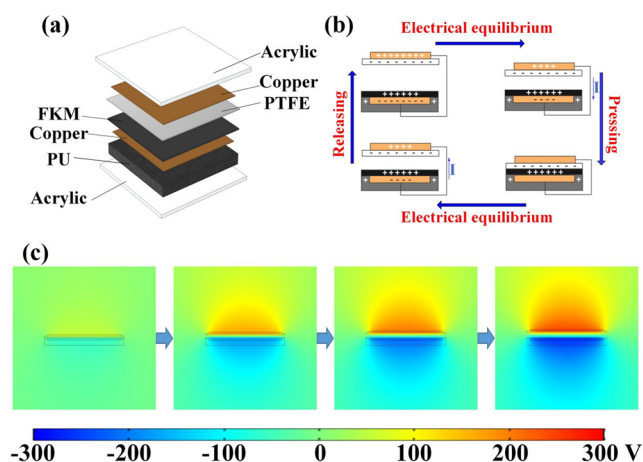

Figure 2. (a) Internal structure and material composition of the stacked FKM/PU TENG. (b) Mechanism of the stacked FKM/PU TENG. (c) Corresponding potential distribution on the conductive copper simulated by the software COMSOL.

unlike the previous cushion, the PU is attached to the FKM. When Plates A and B squeeze each other, the PU is also involved in the triboelectrification. The working principle is shown in Figure 2b. When the PTFE contacted and began to squeeze the FKM of Plate B, the PU is compressed and deforms, and the electrons on the two triboelectric materials FKM and PU of Plate B transfer to the PTFE. During the extrusion, the PU deformation increases, and the electrons on the PU continue to transfer to the PTFE. When the PU reaches the deformation limit, Plate A cannot continue to squeeze the lower plate, and the contact between the FKM and PTFE is closer, which promotes electron transfer between the FKM and PTFE. Finally, the PTFE of Plate A has more negative charges, and the PU and FKM of Plate B have more

positive charges. When Plate A contacts and squeezes the lower plate, the external circuit between the copper electrodes on the plate generates an electrostatically induced current from the top to the bottom. When Plate A ends the extrusion and separates from Plate B, a current is induced in the opposite direction in the external circuit. By repeating this process, the TENG can output AC electric energy. Figure 2c displays the potential distribution of the conductive copper on Plates A and B simulated by the software COMSOL. Comparing with Figure 2b shows the conductive copper attains its maximum potential as Plates A and B separate.

2.2. The Output Performance. To test the output performance of the stacked FKM/PU TENG, the reciprocating mechanism is used to simulate the impacting of Plate A on Plate B, as shown in Figure 3a and Figure S1. The output parameters of the stacked TENG under different extrusion conditions are measured by adding a square acrylic sheet (thickness: 3 mm) between the plates and adjusting the fixed position of the flange seat (offset distance: 1−2 mm). Several working modes of the stacked FKM/PU TENG are tested according to the initial position, the number of additional acrylic plates, and the offset. The following conditions are tested: noncontact ($N = 0, 1$), contact ($N = 2$), extrusion ($N = 3, 4$), impact ($N = 5, 5 + 1$ mm), and maximum compression. Maximum compression is defined as 5 additional acrylic plates. The offset distance of the flange seat is increased from 1 mm until it is almost impossible for the reciprocating motion to continue, and the stacked FKM/PU TENG reaches its limit.

In Figure 3b,c, the open-circuit voltage V_{OC} and short-circuit current I_{SC} of the stacked FKM/PU TENG increase simultaneously with increasing driving frequency (1−3 Hz) at $N = 5$. When the driven frequency is 1 Hz, the maximum V_{OC} of the TENG is 220 V and I_{SC} is 22.4 μA. Enhancing the frequency to 3 Hz raises the maximum instantaneous V_{OC} to 431 V and the I_{SC} to 68.1 μA. Under maximum compression, the stacked TENG reached its limits of 661 V and 71.2 μA. This can be explained by the improvement of the charge transfer rate related to the contact frequency. The promotion in force (refer to Table S1: 1.4−4.2 N) presented a stronger collision between plates. Thus, tribo-layers accumulated more electrical charge. The deformation of PU prolongs the contact and extra induced charge, optimizing the effect of the TENG.[17,19] In Figure S2a,b, with the simple use of PU as the cushion (as shown in Figure 1c) for processing, the maximum I_{SC} can only reach 40.6 μA, while the stacked FKM/PU TENG is much better than the former. In addition, compared with the amount of transferred charge in 1 s, the FKM TENG with PU cushion only reaches 1.14 μC, which is also behind this work (2.23 μC). Based on the comparison results, the stacked FKM/PU TENG has much higher output performance than the FKM-TENG and PU-TENG, even greater than the sum of the two.

Next, in order to observe the influence of the deformation degree of PU on the output performance, we set the driving frequency to 3 Hz, changed the number of additional acrylic plates and the offset distance of the flange seat, and measured V_{OC} and the total transferred charge each second under the different conditions. Figure 3d,e shows that when FKM and PTFE are not in contact and charges are only driven through the induction between FKM and PTFE, V_{OC} is not more than 100 V, and the total transferred charge is not more than 750 nC. Increasing the number of acrylic plates to $N = 2$ brings the FKM and PTFE into contact, and V_{OC} and the total transferred
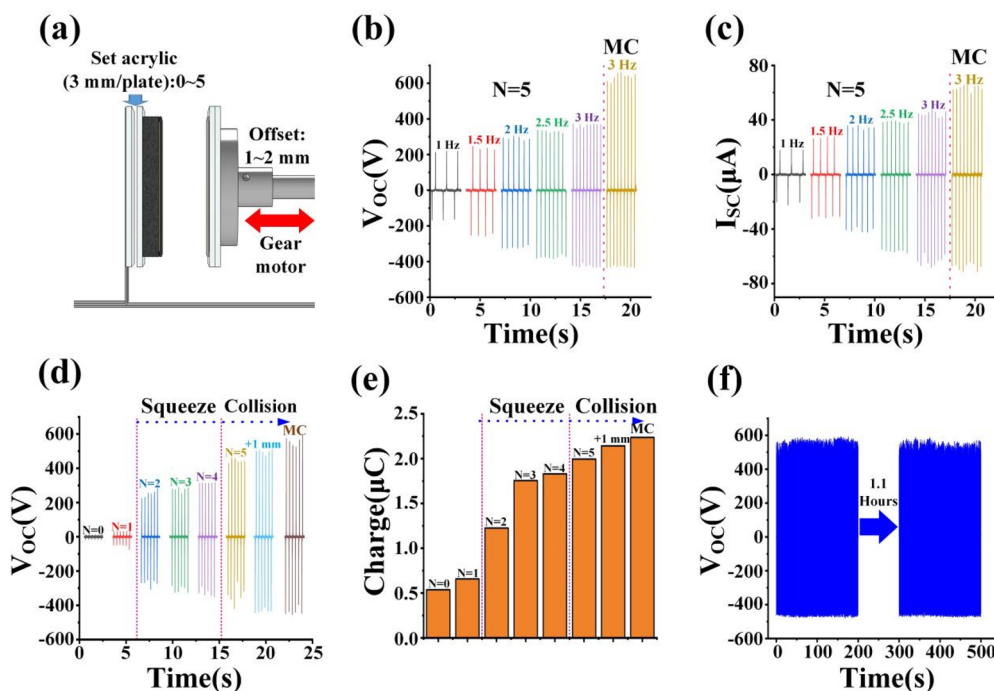
Figure 3. (a) Working conditions of the TENG. (b) V_{OC} and (c) short-circuit current I_{SC} at $N = 5$ and maximum compression. (d) V_{OC} under different conditions. (e) Total transferred charge under different conditions. (f) Durability.
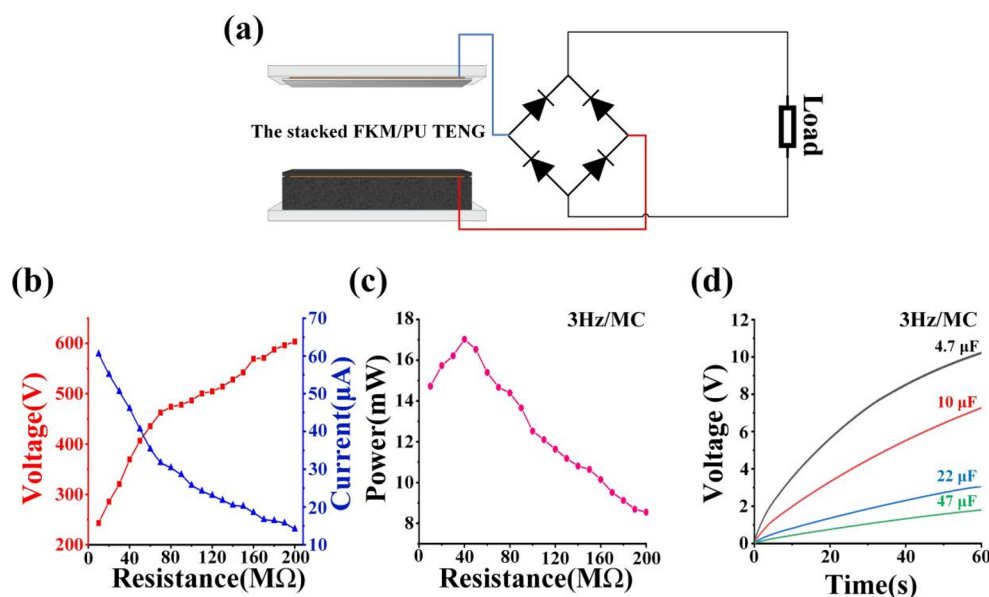

Figure 4. (a) Circuit diagram of the TENG. (b) Output current and voltage and (c) output power under different loads. (d) Voltages of capacitors charged by the stacked FKM/PU TENG.

charge increase. When N is equal to 3 or 4, the PU is compressed. The stacked FKM/PU TENG is under extrusion, making V_{OC} reach approximately 300 V, and the total transferred charge increases by approximately 0.53 μC compared with $N = 2$. This is because after the compression and deformation, the PU is also involved in the electron transfer and improves the effect of contact between the FKM and PTFE. At $N \geq 4$, which approaches the compression limit, the compressed PU begins to harden, making the whole process of contact, compression, and separation more difficult. Driven by the linear motor, Plates A and B collide continuously, and V_{OC} and the total transferred charge further

increase. At $N = 5 + 1$ mm, V_{OC} is approximately 500 V and the total transferred charge reaches 2.14 μC. When the flange offset is increased to the critical state, V_{OC} becomes maximum and the total transferred charge reaches 2.23 μC. Therefore, increasing extrusion also improves the output performance of the stacked FKM/PU TENG. The open-circuit voltage and transferred charge under different extrusion conditions show that the TENG can regulate its output better than the traditional design. The degree of elastic deformation based on PU affects the contact effect. In addition, the increase in compression increases the amount of induced charge of the PU itself, further improving the output. Durability is also a very
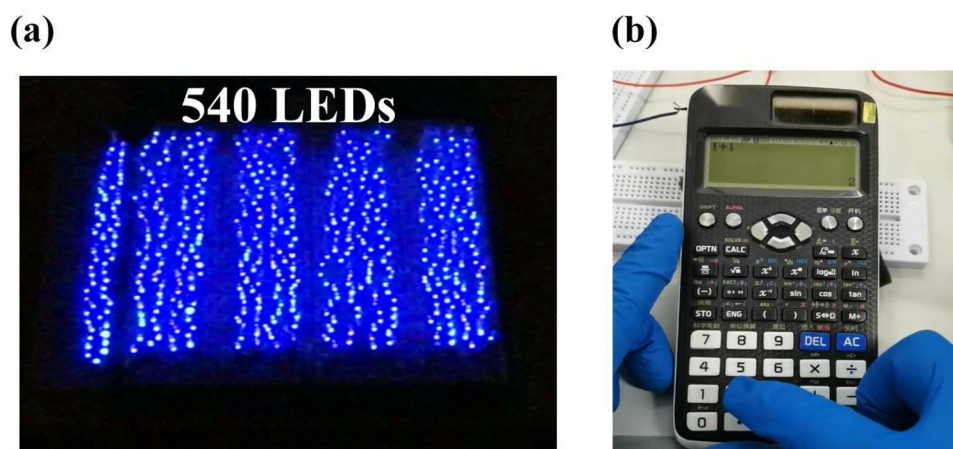
Figure 5. Stacked FKM/PU TENG driving (a) 540 LEDs and (b) a calculator. LED: light-emitting diode.

important factor for TENGs. After enduring long-term and intense contact, TENGs only composed of rigid triboelectric materials are often abraded, which weakens the output. The TENG in this work has elastomer assistance from PU, which offers a buffer and reduces the FKM surface abrasion. Its good stability is shown in Figure 3f. At 3 Hz, V_{OC} is still in its initial state 1.1 h later, and no obvious attenuation occurs during impact.

2.3. Practical Application. To further demonstrate the application prospects of this TENG, it is connected to a loading circuit through a rectifier bridge to observe its operation. The working circuit is shown in Figure 4a. The voltage, current, and output power for different loads are estimated. At resistances from 10 MΩ to 200 MΩ, the output voltage increases from 250 to 600 V, and the output current decreases from 60 μA to 14 μA as the external resistance increases, as shown in Figure 4b,c. At 40 MΩ, the device reaches its maximum power of 17.02 mW. Therefore, the power density can reach 49.62 W/m³, which means it achieves higher power than previous designs.[17,19−21]

A series of capacitors (4.7 μF, 10 μF, 22 μF, 47 μF) are then used to measure the charging ability of the stacked FKM/PU TENG at maximum extrusion, as shown in Figure 4d. Within 60 s, the 4.7 μF capacitor is charged to 10.2 V, and the 47 μF capacitor is charged to 1.8 V. Generally, the output of TENGs without material optimization is weak. However, this work adopts orderly stacking of multiple elastomers and non-elastomers to form a multilayer structure that makes the FKM/PU TENG perform better than designs specially optimized at the material level. The stacked FKM/PU TENG can also charge quickly in a short time, which greatly improves its practicability. Therefore, regardless of the output power or charging speed, the stacked FKM/PU TENG exhibits great potency in practical application.

Under the same working conditions, the TENG can drive 540 blue commercial LEDs and achieve good brightness (shown in Figure 5a and Video S2). Moreover, in Figures 5b and S3 and Video S3, a Casio fx-991cnx calculator is driven to perform simple addition calculations. These actual driving examples with two low-power-consumption loads verify the above conclusions. This fully indicates that this novel TENG introduced in this work can have a role in collecting discrete mechanical energy.

3. DISCUSSION

This work has proposed a new design of TENG based on stacking FKM and PU to form a stacked FKM/PU TENG. This TENG incorporates the merits of the PU and FKM into a single triboelectric material. Preparing this TENG is simple and inexpensive. Powered by a reciprocating mechanism, the stacked FKM/PU TENG generates a short-circuit current of up to 71.2 μA and open-circuit voltage as high as 661 V. The degree of PU deformation changes as acrylic plates are added to change the extrusion environment, so the output voltage and total transferred charge of the TENG gradually increase from 11.2 to 589.9 V and 0.53 μC to 2.24 μC, respectively. Even after intense impact, the friction layer consisting of PTFE is not significantly worn, and V_{OC} remains above 500 V. Under a load of 40 MΩ, the FKM/PU TENG achieves a maximum instantaneous output power of 17.02 mW and power density of 49.62 W/m³. Within 60 s, the low-frequency driven stacked FKM/PU TENG can achieve a voltage of 10.2 V across a 4.7 μF capacitor. Such good output characteristics are attributed to not only the triboelectric characteristics of FKM and PTFE but also the synergy of the elastomer and nonelastomer in the stacked structure. This structure improves the contact, extrusion, and collision effects of the working TENG. Increasing the degree of extrusion increases the amount of induced charge in the PU layer, which also improves the performance of the stacked FKM/PU TENG. Thus, the stacked structure enables the TENG to have a better output than the FKM-TENG and PU-TENG combined. This paper also carried out an actual loading test. The stacked FKM/PU TENG performs outstandingly in lighting 540 commercial LEDs and driving calculators for simple computations, demonstrating a strong application potential. This TENG can help future development of energy collection and sensing technology.

■ ASSOCIATED CONTENT

Ⓢ Supporting Information

The Supporting Information is available free of charge at https://pubs.acs.org/doi/10.1021/acsomega.3c00970.

> Supplementary Figure S1: The experiment platform. Supplementary Table S1: Parameter list of reciprocating mechanism. Supplementary Figure S2: The I_{SC} of (a) FKM TENG with PU cushion and (b) this work. Supplementary Figure S3: The capacitance (47 μF)

charging−discharging curve of the TENG driven calculator (PDF)

Supplementary video 1: Experiment platform for the stacking FKM/PU TENG (MP4)

Supplementary video 2: The stacked FKM/PU TENG drives 540 LEDs (MP4)

Supplementary video 3: The stacked FKM/PU TENG drives calculator (MP4)

■ AUTHOR INFORMATION

Corresponding Authors

Wuwei Feng − *School of Marine Engineering Equipment, Zhejiang Ocean University, Zhoushan 316022, China;* Email: fengwuwei@163.com

Zhenhua Li − *School of Marine Engineering Equipment, Zhejiang Ocean University, Zhoushan 316022, China;* Email: lizh76095@zjou.edu.cn

Authors

Yuxiang Su − *School of Marine Engineering Equipment, Zhejiang Ocean University, Zhoushan 316022, China; School of Electrical Engineering, Southwest Jiaotong University, Chengdu 611756, China;* Present Address: School of Marine Engineering Equipment, Zhejiang Ocean University, Zhoushan 316022, China; orcid.org/0000-0002-8797-5884

Anguo Liu − *School of Marine Engineering Equipment, Zhejiang Ocean University, Zhoushan 316022, China*

Yunqing Gu − *School of Marine Engineering Equipment, Zhejiang Ocean University, Zhoushan 316022, China*

Xiaonan Su − *School of Marine Engineering Equipment, Zhejiang Ocean University, Zhoushan 316022, China*

Guanyu Dai − *School of Marine Engineering Equipment, Zhejiang Ocean University, Zhoushan 316022, China*

Yilei Shao − *School of Marine Engineering Equipment, Zhejiang Ocean University, Zhoushan 316022, China*

Liping Wan − *School of Marine Engineering Equipment, Zhejiang Ocean University, Zhoushan 316022, China*

Haohan Fang − *School of Marine Engineering Equipment, Zhejiang Ocean University, Zhoushan 316022, China*

Complete contact information is available at: https://pubs.acs.org/10.1021/acsomega.3c00970

Author Contributions

The manuscript was written through contributions of all authors. All authors have given approval to the final version of the manuscript. Anguo Liu, Xinyao Zhang, and Liping Wan conceived and designed the TENG. Xiaonan Su, Yilei Shao, and Zhenhua Li conducted the electrical measurements and data analysis. The article was finished by Yuxiang Su with the teamwork from all coauthors. Guanyu Dai, Wuwei Feng, and Haohan Fang provided some suggestions on the experiment.

■ REFERENCES

(1) Kim, W.; Bhatia, D.; Jeong, S.; Choi, D. Mechanical energy conversion systems for triboelectric nanogenerators: Kinematic and vibrational designs. *Nano Energy* **2019**, *56*, 307−321.

(2) Li, C.; Zhu, Y.; Sun, F.; Jia, C.; Zhao, T.; Mao, Y.; Yang, H. Research progress on triboelectric nanogenerator for sports applications. *Energies* **2022**, *15*, 5807.

(3) Wang, Z. L.; Chen, J.; Lin, L. Progress in triboelectric nanogenerators as a new energy technology and self-powered sensors. *Energy Environ. Sci.* **2015**, *8*, 2250−2282.

(4) Luo, J.; Wang, Z. L. Recent advances in triboelectric nanogenerator based self-charging power systems. *Energy Storage Mater.* **2019**, *23*, 617−628.

(5) Dong, S.; Xu, F.; Sheng, Y.; Guo, Z.; Pu, X.; Liu, Y. Seamlessly knitted stretchable comfortable textile triboelectric nanogenerators for E-textile power sources. *Nano Energy* **2020**, *78*, 105327.

(6) Gao, Y.; Li, Z.; Xu, B.; Li, M.; Jiang, C.; Guan, X.; Yang, Y. Scalable core−spun coating yarn-based triboelectric nanogenerators with hierarchical structure for wearable energy harvesting and sensing via continuous manufacturing. *Nano Energy* **2022**, *91*, 106672.

(7) Jing, T.; Xu, B.; Yang, Y.; Li, M.; Gao, Y. Organogel electrode enables highly transparent and stretchable triboelectric nanogenerators of high power density for robust and reliable energy harvesting. *Nano Energy* **2020**, *78*, 105373.

(8) Xing, F.; Jie, Y.; Cao, X.; Li, T.; Wang, N. Natural triboelectric nanogenerator based on soles for harvesting low-frequency walking energy. *Nano Energy* **2017**, *42*, 138−142.

(9) Cao, B.; Wang, P.; Rui, P.; Wei, X.; Wang, Z.; Yang, Y.; Tu, X.; Chen, C.; Wang, Z.; Yang, Z.; Jiang, T.; Cheng, J.; Wang, Z. L. Broadband and output-controllable triboelectric nanogenerator enabled by coupling swing-rotation switching mechanism with potential energy storage/release strategy for low-frequency mechanical energy harvesting. *Adv. Energy Mater.* **2022**, *12*, 2202627.

(10) Cheng, J.; Zhang, X.; Jia, T.; Wu, Q.; Dong, Y.; Wang, D. Triboelectric nanogenerator with a seesaw structure for harvesting ocean energy. *Nano Energy* **2022**, *102*, 107622.

(11) Hong, H.; Yang, X.; Cui, H.; Zheng, D.; Wen, H.; Huang, R.; Liu, L.; Duan, J.; Tang, Q. Self-powered seesaw structured spherical buoys based on a hybrid triboelectric−electromagnetic nanogenerator for sea surface wireless positioning. *Energy Environ. Sci.* **2022**, *15*, 621−632.

(12) Guo, Y.; Chen, Y.; Ma, J.; Zhu, H.; Cao, X.; Wang, N.; Wang, Z. L. Harvesting wind energy: A hybridized design of pinwheel by coupling triboelectrification and electromagnetic induction effects. *Nano Energy* **2019**, *60*, 641−648.

(13) Huang, L.-b.; Xu, W.; Bai, G.; Wong, M.-C.; Yang, Z.; Hao, J. Wind energy and blue energy harvesting based on magnetic-assisted noncontact triboelectric nanogenerator. *Nano Energy* **2016**, *30*, 36−42.

(14) Kim, D.; Tcho, I.-W.; Choi, Y.-K. Triboelectric nanogenerator based on rolling motion of beads for harvesting wind energy as active wind speed sensor. *Nano Energy* **2018**, *52*, 256−263.

(15) Zhang, J.; Zheng, Y.; Xu, L.; Wang, D. Oleic-acid enhanced triboelectric nanogenerator with high output performance and wear resistance. *Nano Energy* **2020**, *69*, 104435.

(16) Salauddin, M.; Rana, S. M. S.; Sharifuzzaman, M.; Rahman, M. T.; Park, C.; Cho, H.; Maharjan, P.; Bhatta, T.; Park, J. Y. A novel MXene/Ecoflex nanocomposite-coated fabric as a highly negative and stable friction layer for high-output triboelectric nanogenerators. *Adv. Energy Mater.* **2021**, *11*, 2002832.

(17) Liu, Y.; Zheng, Y.; Wu, Z.; Zhang, L.; Sun, W.; Li, T.; Wang, D.; Zhou, F. Conductive elastic sponge-based triboelectric nanogenerator (TENG) for effective random mechanical energy harvesting and ammonia sensing. *Nano Energy* **2021**, *79*, 105422.

(18) Zou, H.; Zhang, Y.; Guo, L.; Wang, P.; He, X.; Dai, G.; Zheng, H.; Chen, C.; Wang, A. C.; Xu, C.; Wang, Z. L. Quantifying the triboelectric series. *Nat. Commun.* **2019**, *10*, 1427.

(19) Xia, K.; Fu, J.; Xu, Z. Multiple-frequency high-output triboelectric nanogenerator based on a water balloon for all-weather water wave energy harvesting. *Adv. Energy Mater.* **2020**, *10*, 2000426.

(20) Hao, S.; Jiao, J.; Chen, Y.; Wang, Z. L.; Cao, X. Natural wood-based triboelectric nanogenerator as self-powered sensing for smart homes and floors. *Nano Energy* **2020**, *75*, 104957.

(21) Xiang, H.; Yang, J.; Cao, X.; Wang, N. Flexible and highly sensitive triboelectric nanogenerator with magnetic nanocomposites for cultural heritage conservation and human motion monitoring. *Nano Energy* **2022**, *101*, 107570.